Metamorphism and partial melting of ordinary chondrites: calculated phase equilibria

T. E. Johnson[a,*], G. K. Benedix[a,b] & P. A. Bland[a]

[a] *Department of Applied Geology, The Institute for Geoscience Research (TIGeR), Curtin University, GPO Box U1987, Perth WA 6845, Australia*

[b] *Department of Earth and Planetary Sciences, Western Australia Museum, 49 Kew Street, Welshpool, WA 6986, Australia*

* Corresponding author at: Department of Applied Geology, The Institute for Geoscience Research (TIGeR), Curtin University, GPO Box U1987, Perth WA 6845, Australia. Tel: +61 8 9266 7332; fax: +61 8 9266 3153.

E-mail address: tim.johnson@curtin.edu.au (Tim Johnson).

Short title: **Phase equilibria modelling of ordinary chondrites**

ABSTRACT

Constraining the metamorphic pressures (*P*) and temperatures (*T*) recorded by meteorites is key to understanding the size and thermal history of their asteroid parent bodies. New thermodynamic models calibrated to very low *P* for minerals and melt in terrestrial mantle peridotite permit quantitative investigation of high-*T* metamorphism in ordinary chondrites using phase equilibria modelling. Isochemical *P–T* phase diagrams based on the average composition of H, L and LL chondrite falls and contoured for the composition and abundance of olivine, ortho- and clinopyroxene, plagioclase and chromite provide a good match with values measured in so-called equilibrated (petrologic type 4–6) samples. Some compositional variables, in particular Al in orthopyroxene and Na in clinopyroxene, exhibit a strong pressure dependence when considered over a range of several kilobars, providing a means of recognising meteorites derived from the cores of asteroids with radii of several hundred kilometres, if such bodies existed at that time. At the low pressures (<1 kbar) that typified thermal metamorphism, several compositional variables are good thermometers. Although those based on Fe–Mg exchange are likely to have been reset during slow cooling, those based on coupled substitution, in particular Ca and Al in orthopyroxene and Na in clinopyroxene, are less susceptible to retrograde diffusion and are potentially more faithful recorders of peak conditions. The intersection of isopleths of these variables may allow pressures to be quantified, even at low *P*, permitting constraints on the minimum size of parent asteroid bodies. The phase diagrams predict the onset of partial melting at 1050–1100 °C by incongruent reactions consuming plagioclase, clinopyroxene and orthopyroxene, whose compositions change abruptly as melting proceeds. These predictions match natural observations well and support the view that type 7 chondrites represent a suprasolidus continuation of the established petrologic types at the extremes of thermal metamorphism. The results suggest phase equilibria modelling has potential as a powerful quantitative tool in investigating, for example, progressive oxidation during metamorphism, the

degree of melting and melt loss or accumulation required to produce the spectrum of differentiated meteorites, and whether the onion shell or rubble pile model best explains the metamorphic evolution of asteroid parent bodies in the early solar system.

Keywords: meteorite; ordinary chondrite; metamorphism; phase equilibria modelling; mineral chemistry.

1. Introduction

Chondritic meteorites are the oldest known rocks containing components whose age defines that of the solar system (Allegre et al., 1995; Patterson, 1956). Their study provides clues critical to understanding the formation of the sun and planets, and their arrival from outer space has had a profound impact on the evolution of life on Earth (Scott, 2007; Sleep et al., 1989; Suess, 1965; Trieloff et al., 2003; Urey, 1962). Ordinary chondrites are by far the most abundant type of meteorite, comprising 80% of all that fall to Earth. Along with composition (H, L and LL), metamorphic grade, or petrologic type, is a primary variable by which ordinary chondrites are classified (Van Schmus and Wood, 1967). More accurately constraining the metamorphic history of chondrites and their parent bodies is key to better understanding the early evolution of the solar system.

Based on the U–Pb systematics of phosphates within ordinary chondrites, the peak of thermal metamorphism is constrained to the interval 4.56–4.50 Ga (Göpel et al., 1994), in which the two viable heat sources were decay of short-lived radionuclides, mainly ^{26}Al (Hutcheon and Hutchison, 1989; Minster and Allègre, 1979), and frictional heating due to impacts (Ciesla et al., 2013; Rubin, 1995). Two plausible end-member hypotheses have been proposed to explain the thermal and accretionary histories of the parent asteroid bodies from which ordinary chondrites

were derived (Harrison and Grimm, 2010; McSween and Patchen, 1989; Scott and Rajan, 1981). The 'onion-shell' model requires that parent bodies remained more-or-less undisturbed during metamorphism and subsequent cooling. In this model, in which the contribution from impact heating may have been small, metamorphic temperature (*T* and petrologic type) and pressure (*P*) should be positively correlated, and *T* and cooling rate (*S*) inversely correlated (Göpel et al., 1994; Harrison and Grimm, 2010; Herndon and Herndon, 1977; Minster and Allègre, 1979; Trieloff et al., 2003). The 'rubble-pile' hypothesis involves syn-metamorphic fragmentation and reassembly of parent bodies before they had cooled (Harrison and Grimm, 2010; McSween and Patchen, 1989; Scott et al., 2014; Scott and Rajan, 1981). In this scenario *T*, *P* and *S* may exhibit no clear correlations and the contribution of impact heating may have been dominant.

So-called equilibrated (type 4–7) ordinary chondrites are fine-grained metamorphosed ultramafic rocks characterised by increasing grain size (from a few microns or less in type 4 to several tens of microns in types 6 and 7) and textural integration between matrix and chondrules (Dodd et al., 1967; Huss et al., 2006; Van Schmus and Wood, 1967). Equilibrated ordinary chondrites contain mineral assemblages comprising variable abundances of the silicate minerals olivine, orthopyroxene, clinopyroxene and plagioclase with Fe–Ni metal (taenite–kamacite), sulphide (troilite), chromite, phosphate (apatite and merrilite) and accessory phases (Dunn et al., 2010a; Huss et al., 2006; Tait et al., 2014). Although olivine is equilibrated (i.e. shows no compositional zoning) by type 4, pyroxene may not be compositionally equilibrated until type 5 (Dodd, 1969; Huss et al., 2006; Van Schmus and Wood, 1967). Based largely on experimentally calibrated equilibria, principally two-pyroxene thermometry, temperatures in type 4–6 ordinary chondrites are generally estimated at between 500 °C and 1000 °C (Dodd, 1981; Mare et al., 2014; McSween and Patchen, 1989; McSween et al., 1988; Slater-Reynolds and McSween Jr, 2005). However, it is unclear to what degree these thermometers record equilibrium at peak metamorphic conditions, or rather reflect incomplete re-equilibration of primary (igneous) compositions and/or retrograde resetting of peak metamorphic compositions during cooling

(McSween and Patchen, 1989). Silicate partial melting in type 7 chondrites is evidence for metamorphic temperatures in excess of ~1050–1150 °C (Hutchison, 2004; Jurewicz et al., 1993; Keil, 2000; McSween and Patchen, 1989; Tait et al., 2014).

Metamorphic pressures are much harder to constrain, but are generally thought to be less than 1 kbar (Dodd, 1969; McSween and Patchen, 1989). Assuming a constant density of 3300–3400 kg/m^3, pressures of 1 kbar correspond to maximum depths of around 250 km and derivation from bodies similar in size to, or larger than, Vesta. However, significantly higher pressures up to and in excess of 10 kbar have been suggested on the basis of structural parameters in clinopyroxene (Pletchov et al., 2005; Zinovieva et al., 2006).

Equilibrium phase diagrams calculated for specified rock compositions have become the method of choice in constraining the *P–T* history of metamorphic rocks on Earth, where the approach is routinely applied to both subsolidus rocks and those that partially melted (migmatites) under the most extreme metamorphic conditions (Kelsey and Hand, 2015; Korhonen et al., 2014; White et al., 2014). However, to date such studies have concentrated on crustal rocks. Building on models developed in the simple $CaO–MgO–Al_2O_3–SiO_2$ system (Green et al., 2012a; Green et al., 2012b), thermodynamic models describing non-ideal activity–composition relations for solid solution minerals (olivine, orthopyroxene, clinopyroxene, garnet, plagioclase, spinel, chromite) and silicate melt in anhydrous peridotite have recently been calibrated in the expanded $Na_2O–CaO–FeO–MgO–Al_2O_3–SiO_2–Fe_2O_3–Cr_2O_3$ (NCFMASOCr) chemical system (Jennings and Holland, 2015). Although designed specifically to investigate equilibria in fertile upper mantle, including its partial melting to produce basaltic primary (oceanic) crust, the solution models are calibrated down to very low pressures (1 bar) allowing, for the first time, a quantitative investigation of phase equilibria in stony meteorites using a modern petrological approach.

Here we present subsolidus and suprasolidus *P–T* phase relations for ordinary chondrites, including the calculated abundance and composition of the main minerals. We compare and

129 contrast the results with existing data to assess the viability of the phase equilibria modelling
130 approach to extraterrestrial rocks. We discuss how the method might be used to better constrain
131 metamorphic pressures and temperatures and in the quantitative investigation of some key
132 processes operating during the early evolution of the solar system.
133
134
135 **2. Samples and methods**
136
137 Bulk rock data from more than 1000 meteorites compiled by Nittler et al. (2004)
138 demonstrates that, although exhibiting considerable variability and overlap, H (n = 195), L (n =
139 217) and LL (n = 53) ordinary chondrites define distinct compositional groups for some major
140 elements (Fig. 1; Supplementary Fig. S1). Although, by definition, class H chondrites have the
141 highest elemental Fe abundances, they also have the highest concentrations of metallic Fe. After
142 excluding metallic Fe and that associated with sulphides, H chondrites have the lowest FeO
143 contents and *X*(Fe) (=molar FeO/FeO + MgO), and LL the highest (Nittler et al., 2004) (Fig. 1).
144 Importantly, there is a clear distinction between meteorite finds and falls, in particular with
145 respect to FeO. This is most pronounced for H chondrites, for which the average of falls contains
146 significantly less FeO (~10 wt%) than the average of all analysed H chondrites (~13 wt%),
147 consistent with terrestrial weathering and concomitant oxidation of metallic Fe in meteorite finds
148 (Nittler et al., 2004).
149 For representative compositions for phase equilibria modelling we use the average
150 composition of meteorite falls for H (n = 34), L (n = 58) and LL (n = 12) chondrites (see Table 1,
151 in mol.%), which define a linear trend from H [FeO = 10.05 wt% FeO, *X*(Fe) = 0.19] through L
152 [FeO = 14.62 wt% FeO, *X*(Fe) = 0.25] to LL [FeO = 17.74 wt% FeO, *X*(Fe) = 0.28] (Fig. 1).
153 Calculations assume equilibration with metallic Fe and, consequently, no Fe_2O_3. Metallic Fe and
154 the Fe in sulphides (FeS), reported separately in the Nittler et al. (2004) database, were assumed

to be present in excess and excluded from the modelled bulk compositions. Also excluded was a small amount of CaO (3.33 times molar P_2O_5) to account for minor apatite.

Phase diagrams were computed using the software THERMOCALC V.3.40i (Powell and Holland, 1988) and the internally consistent thermodynamic data set of Holland and Powell (2011) (ds63 dataset generated on 24/01/15). Calculations consider the phases garnet (g), olivine (ol), orthopyroxene (opx), clinopyroxene (cpx), plagioclase (pl), spinel *sensu lato* [in which we make a distinction between potentially coexisting subsolvus compositions rich in Cr and Fe (chromite, cm) and aluminium (spinel *sensu stricto*, sp)] and silicate melt (liq). Activity–composition models follow Jennings and Holland (2015), but with ferric iron excluded. Calculated phase diagrams were contoured for the abundance and composition of phases using TC Investigator (Pearce *et al.*, 2015). We first present phase relations to high pressures (15 kbar), allowing theoretical consideration of metamorphism in the core of asteroids with radii approaching a thousand kilometres (although we make no claim that such large asteroids existed at that time).

3. Results

3.1. Equilibrium assemblages

Isochemical *P–T* phase diagrams for the average composition of H, L and LL ordinary chondrite falls from 700–1200 °C and 0.001–15 kbar are shown in Fig. 2. While there are subtle differences, all phase diagrams have a similar topology. For the temperature range considered, the subsolidus equilibrium assemblage at pressures less than 8–9 kbar is olivine, orthopyroxene, clinopyroxene, plagioclase and chromite (shown in bold on Fig. 2). Although aluminous spinel is predicted to be stable, it occurs only at temperatures lower than those modelled here (i.e. <700 °C). At pressures above 8–9 kbar, no chromite is predicted; at pressures above around 9 kbar (at

700 °C) to 12 kbar (at 1100 °C), plagioclase does not occur. At the highest pressures and lowest temperatures modelled, garnet is stable, its stability field extending to significantly lower *P* in type LL relative to type H (Fig. 2).

For each of the average compositions, the prograde onset of partial melting occurs at ~1050 °C at low *P* (<1 kbar) to ~1150 °C at 12–13 kbar, where the solidus is intersected by the disappearance of plagioclase to higher pressures (Fig. 2). After crossing the solidus up-grade at pressures below 12–13 kbar, partial melting occurs by incongruent reactions consuming plagioclase, clinopyroxene and orthopyroxene. In H and L chondrites, first plagioclase then clinopyroxene then orthopyroxene are exhausted as reaction proceeds (Fig. 2a,b). This sequence is followed for the average LL chondrite composition except at low *P* (<2 kbar), where plagioclase is predicted to disappear a few degrees before clinopyroxene is exhausted (Fig. 2c).

For the average H composition, a complex series of sub- and suprasolidus fields between ~3–10 kbar and ~1025–1150 °C define a solvus in which two clinopyroxenes (Ca-rich 'augite' and Ca-poor 'pigeonite') coexist (Fig. 2a). A similar solvus is predicted for the average L composition, albeit across a smaller *P–T* region (Fig. 2b). No solvus is present for the average LL composition (Fig. 2c).

3.2. Abundance of minerals

The calculated abundance (in mol.% on a one oxide basis to approximate vol.%) of the main silicate minerals olivine, orthopyroxene, clinopyroxene and plagioclase for the average H, L, and LL compositions is shown in Fig. 3. For simplicity, where a solvus exists (i.e. for H and L; Fig. 2a,b), the combined abundance of both clinopyroxenes is shown. At subsolidus conditions, the abundance of olivine decreases with increasing pressure and is lowest for H (from ~44% at low *P* to 38% at high *P*) and highest for LL chondrites (~57% at low *P* to 51% at high *P*). The abundance of orthopyroxene increases with pressure and decreases with increasing

temperature in the subsolidus region. Overall the average H chondrite contain 35–40% orthopyroxene at temperatures below 1000 °C, around 5% more orthopyroxene than L and 10% more than LL chondrites. The abundance of clinopyroxene in the subsolidus region increases both with pressure and, at high *P*, temperature, varying in H from ~5% at low *P* and *T* (<1 kbar, 700 °C) to 40% at high *P* and *T* (12–15 kbar, 1150 °C). The absolute abundance of clinopyroxene in the average H chondrite at any specific *P* and *T* is higher than in L, which is in turn higher than in LL (Fig. 3). The abundance of plagioclase shows little variation between the compositional types and, in the subsolidus region, is strongly pressure dependent, varying from 10–12% at low pressures and disappearing at pressures of 10–12 kbar (Fig. 2 & 3). For all compositions, on crossing the solidus at any fixed *P* the abundance of olivine increases whereas that of the other main silicate minerals decreases with increasing temperature. This reflects consumption of plagioclase, clinopyroxene and orthopyroxene by incongruent reactions producing melt and olivine. The abundance of chromite (not shown), which decreases slightly with increasing pressure and increases slightly on heating beyond the solidus, is <0.5% in all compositional groups (H, L and LL).

3.3. Composition of minerals

Although the absolute composition of phases can vary significantly between compositional types, in particular *X*(Fe) in ferromagnesian minerals that is a function of bulk *X*(Fe), the relative changes in composition with *P* and *T* are almost identical. We illustrate these changes with reference to the average L chondrite composition, for which Fig. 4 show phase diagrams from 0.001 to 15 kbar contoured for mineral compositions. Equivalent diagrams for H and LL chondrites are given in Supplementary material (Figs S2 & S3, respectively). The compositional variables for the minerals in the model system are detailed in the caption to Fig. 4 and summarised as follows: *X*(Fe) = atomic Fe/(Fe + Mg); in pyroxenes, *X*(Al) = tetrahedral Al

cations per formula unit (c.p.f.u.) on a 6 oxygen basis; in orthopyroxene X(Ca) = Ca c.p.f.u. (6 oxygen); in clinopyroxene X(Na) = Na c.p.f.u. (6 oxygen); in plagioclase X(Ca) = mole fraction anorthite; in chromite X(Cr) = ½ Cr c.p.f.u. (4 oxygen). For all mineral composition diagrams, the top row shows variables for olivine (a) and chromite (b & c), the second row shows variables for orthopyroxene (d–f), the third row shows variables for clinopyroxene (g–i), and the composition of plagioclase is shown in (j). For simplicity, the composition of clinopyroxene within the solvus region (Fig. 4g–i) is an integrated composition combining both low-Ca and high-Ca clinopyroxene.

The calculated X(Fe) of olivine and orthopyroxene is near constant at all subsolidus pressures and temperatures (~0.20 in olivine and ~0.18 in orthopyroxene for H, ~0.25 and ~0.22 respectively for L and ~0.28 and ~0.24–0.26 respectively for LL); both minerals become significantly more magnesian on crossing the solidus up T. Within the stability field of chromite (P < 8 kbar), subsolidus variations in the Fe and Mg content of the minerals occur predominantly via exchange between clinopyroxene and chromite, whose X(Fe) increase and decrease respectively with increasing temperature. X(Fe) in clinopyroxene decreases with increasing T at higher pressures and on crossing the solidus. Calculated values for X(Al) in clinopyroxene are uniformally low and constant except at the highest P and T where they increase slightly to 0.01–0.02 c.p.f.u.. Values of X(Al) in orthopyroxene show a strong pressure dependence, increasing from 0.02 at low pressures to >0.12 at the highest P and T modelled; at high P subsolidus conditions, X(Al) in orthpyroxene also increases with increasing T. A similarly strong pressure dependence is shown by X(Na) in clinopyroxene, for which calculated values vary from <0.1 c.p.f.u. at low pressures to >0.4 c.p.f.u. at low T and high P; at high pressures this variable decreases with increasing T. Values of X(Ca) in orthopyroxene show little variation between the compositional types. X(Ca) in orthopyroxene increases with temperature and decreases with pressure in the subsolidus region, but decreases on crossing the solidus up T. Throughout most of the subsolidus region, values of X(Ca) in plagioclase and X(Cr) in chromite are strongly pressure

dependent, with absolute values near identical in all compositional types. Plagioclase becomes significantly richer in albite with increasing P [X(Ca) = 0.2 to 0.1] and chromite significantly more depleted in Cr (and enriched in Al). On crossing the solidus plagioclase become much more anorthite-rich [up to X(Ca) of 0.3] before it is exhausted.

4. Discussion

4.1. Calculated vs measured abundance of minerals

Dunn et al. (2010a) measured the modal abundance of minerals in 48 unbrecciated equilibrated (petrologic type 4–6) ordinary chondrites using powder X-ray diffraction (Bland et al., 2004; Cressey and Schofield, 1996). The average abundance (in wt%) of the four main silicate minerals olivine, orthopyroxene, clinopyroxene and plagioclase measured by these authors in H, L and LL chondrites and normalised to 100% is given in Table 2 [see also Hutchison (2004) table 5.1]. These values show good correspondence with those calculated by phase equilibria modelling (Fig. 3), but only at low pressures. This is most clearly illustrated by plagioclase and clinopyroxene, whose measured modes are mostly 10–12 wt% (around 13–15 vol.%) and 8–10 wt% (and vol.%), respectively (Dunn et al., 2010a).

The systematic increase in the mode of olivine and decrease in the mode of orthopyroxene with increasing metamorphic grade in unmelted (type 4 to 6) ordinary chondrites noted by Dunn et al. (2010b) is not reproduced by the modelling. Although these measurements were obviously obtained from meteorites with different bulk compositions, there is no apparent relationship between the changes in mineral modes with grade and the bulk X(Fe) of the meteorite (Dunn et al., 2010b; Nittler et al., 2004). Systematic changes in the abundance of olivine and orthopyroxene with grade are ascribed to progressive oxidation due to reaction with aqueous fluids derived from breakdown of hydrous phases that are common in unequilibrated

285 (type 3) chondrites, in which oxidation of metallic iron reacts with orthopyroxene to produce
286 olivine (Dunn et al., 2010b, McSween and Labotka, 1993; Rubin, 1990). However, we here treat
287 metallic iron as in excess, and a quantitative investigation of this process using isochemical
288 phase diagrams is not possible.
289
290
291 *4.2. Calculated vs measured composition of minerals*
292 The composition of minerals analysed by Dunn et al. (2010b) using electron probe
293 microanalysis (EPMA) in the same samples for which the modal abundances were measured
294 (Dunn et al., 2010a) are also summarised in Table 2 [see also Hutchison (2004) table 5.1]. The
295 measured *X*(Fe) of olivine (fayalite component) and orthopyroxene in ordinary chondrites
296 (Binns, 1970; Dodd, 1969; Dunn et al., 2010b; McSween and Patchen, 1989) show an excellent
297 correspondence with calculated values (compare Table 2 with Figs 4, S2 and S3 a & d).
298 However, measured values of *X*(Fe) in clinopyroxene are generally significantly lower than
299 calculated values within the modelled *P–T* window. For example, the average measured *X*(Fe) in
300 clinopyroxene in the three L6 chondrites analysed by Dunn et al. (2010b) is 0.15, whereas the
301 lowest calculated values (at 1 bar and 700 °C) are around 0.20 (Fig. 4g). A similar feature is
302 shown by LL chondrites, in which *X*(Fe) in clinopyroxene increases from type 4 to type 7,
303 ranging from 0.14 to 0.19 (McSween and Patchen, 1989); the lowest values calculated for the
304 average LL composition are 0.21–0.22 (Fig. S5). By contrast, measured values of *X*(Fe) in
305 chromite (0.81–0.94), which show little clear evidence for systematic change with grade or
306 composition (Bunch et al., 1967), are significantly higher than calculated values (e.g. Fig. 4c).
307 Although this lack of correspondence may point to infelicities in the solution models, the
308 measured values are consistent with diffusive exchange of Fe and Mg during slow cooling to
309 temperatures significantly lower than those modelled (i.e. < or << 700 °C). Retrograde Fe–Mg
310 exchange is near ubiquitous in terrestrial high-grade metamorphic rocks, leading to significant

311 underestimates in peak metamorphic temperatures based on exchange thermometry (Fitzsimons
312 and Harley, 1994).

313 The measured content of Al in orthopyroxene is uniformally low, with both total Al
314 c.p.f.u. (based on 6 oxygens) and tetrahedral Al contents (based on 2 – Si) returning values of
315 0.01–0.03 (Binns, 1970; Dunn et al., 2010b; McSween and Patchen, 1989). These measured
316 values are consistent with calculated values only at low pressure (e.g. Fig. 4e). Measured
317 contents of Ca in orthopyroxene are mainly in the range 0.03–0.05 c.p.f.u. (Binns, 1970; Dunn et
318 al., 2010b; McSween and Patchen, 1989), spanning the range of calculated values (e.g. Fig. 4f).
319 The Ca content of orthopyroxene cores is known to increase with grade (Brearley and Jones,
320 1998; Scott et al., 1986; Tait et al., 2014), consistent with the trend predicted by phase equilibria
321 modelling.

322 Measured concentrations of Na in clinopyroxene are rather constant at around 0.04
323 c.p.f.u. (Dunn et al., 2010b; McSween and Patchen, 1989). These are lower than any calculated
324 values (e.g. Fig. 4i). The composition of plagioclase in ordinary chondrites may be highly
325 variable, which has been interpreted to reflect melting during shock metamorphism, although
326 measured values are commonly albite to sodic oligoclase with X(Ca) 0.09–0.14 (see table 2 in
327 Rubin, 1992). These compositions span calculated subsolidus values, although at low pressures
328 (<1 kbar) the calculated concentrations of the anorthite component are higher (0.17–0.25) than
329 most measured values. The mismatch in the calculated versus measured compositions of Na in
330 clinopyroxene and plagioclase most likely reflects infelicities in the solution models for these
331 phases, in which too much Na is incorporated into clinopyroxene and too little in plagioclase.

332 Measured values of X(Cr) in chromite in type 4 to 6 ordinary chondrites range from 0.78
333 to 0.88 (Bunch et al., 1967) significantly lower than calculated values, at least at $P < 6$ kbar.
334 While some of this variability may be due to Al–Cr exchange, it more likely reflects bulk
335 compositional variations, limitations in the solution model for olivine, which does not currently
336 include Cr, and/or simplifications in the solution model for spinel (Jennings and Holland, 2015).

Finally, type 7 chondrites exhibit features suggesting they experienced extreme metamorphic temperatures and anatexis in which, despite the high temperatures, minerals commonly exhibit pronounced zonation (Dodd et al., 1975; Mittlefehldt and Lindstrom, 2001; Tait et al., 2014). Orthopyroxene grains commonly have rims depleted in Ca and may be overgrown by clinopyroxene, and plagioclase is generally absent from the matrix, occurring only as an interstitial interconnected network in which individual grains have cores richer in anorthite and rims richer in albite orthoclase (Mittlefehldt and Lindstrom, 2001; Tait et al., 2014). These features are consistent with phase equilibria modelling, which predicts that, on crossing the solidus, plagioclase becomes richer in anorthite before being completely dissolved into the melt (e.g. Fig. 4i) and orthopyroxene becomes depleted in Ca (e.g. Fig. 4f) as it and clinopyroxene are consumed.

4.3. Implications for metamorphic pressures and low P *phase diagrams*

It is generally assumed that thermal metamorphism of ordinary chondrites occurred at low pressures of 1–2 kbar or much less (Dodd, 1969; Dodd, 1981; McSween and Patchen, 1989; Tait et al., 2014; cf. Pletchov et al., 2005; Zinovieva et al., 2006). A comparison of the measured abundance and composition of minerals in ordinary chondrites with the results of phase equilibria modelling supports this conclusion. The lack of garnet and presence of plagioclase within equilibrated (type 4–6) ordinary chondrites implies pressures less than 10–12 kbar, and the presence of chromite is consistent with pressures below 9 kbar (Fig. 2). Moreover, the measured abundance of all phases, in particular plagioclase and clinopyroxene, suggests significantly lower *P* (Fig. 3). The Al contents of pyroxene, which are known to have a strong pressure dependence (Binns, 1970; McSween and Patchen, 1989), are uniformally low across all grades. In particular, the low measured contents of Al in orthopyroxene in type 6 chondrites

363 inferred to have been metamorphosed to temperatures approaching 1000 °C (Dunn et al., 2010b;
364 McSween and Patchen, 1989; McSween et al., 1988) are consistent with $P < 1$ bar (e.g. Fig. 4e).
365 Given these constraints, phase diagrams showing mineral compositions from 700–1200
366 °C at low pressures (from 1 bar to 1 kbar) for L chondrites are shown in Fig. 5. Equivalent
367 diagrams for H and LL chondrites are shown in Supplementary material Figs S4 & 5. The most
368 conspicuous feature of Fig. 5 is that most compositional variables have a strong temperature
369 dependence; the only moderate pressure dependence is exhibited by X(Na) in clinopyroxene.
370 Although X(Fe) in clinopyroxene and chromite have potential as thermometers, the measured
371 values probably reflect slow cooling, as argued earlier. The compositions most likely to record
372 peak temperatures (and consequently the best potential thermometers) are X(Ca) and X(Al) in
373 orthopyroxene and X(Na) in clinopyroxene, as incorporation of these elements generally
374 involves coupled substitutions (tschermak and jadeite, respectively), which are much less easily
375 reset during cooling. Although the use of exchange and net transfer equilibria in pyroxenes in
376 constraining metamorphic temperatures is well established, and has been successfully applied to
377 ordinary chondrites (McSween and Patchen, 1989; Olsen and Bunch, 1984), phase equilibria
378 modelling enables visualisation of these and other mineralogical variables as a function of
379 changing pressure, temperature and bulk composition.
380
381
382 **5. Conclusions**
383
384 The chemical system in which modelling can be undertaken (currently NCFMASCrO) is
385 clearly a simplification of natural compositions, which contain additional components (e.g. K, P,
386 Mn, Ni) that will have an effect on phase relations and the composition of minerals. In addition,
387 although differences in elemental concentrations might be small, each meteorite has a unique
388 bulk composition, for which phase equilibria modelling will result in a similarly unique phase

389 diagram in which the predicted abundance and composition of minerals will differ. Nevertheless,
390 the calculated abundance and composition of minerals based on the average compositions of H,
391 L and LL ordinary chondrites generally correspond well with measured values, suggesting phase
392 equilibria modelling has potential as a valuable quantitative tool for investigating metamorphic
393 processes in equilibrated extraterrestrial, as well as terrestrial, rocks.
394 Phase diagrams calculated to high pressure (Fig. 4) provide a means of recognising
395 meteorites potentially derived from parent asteroid bodies many hundred kilometres across, most
396 readily via elevated contents of Al in orthopyroxene and Na in clinopyroxene. However, all
397 studied ordinary chondrites appear to record thermal metamorphism at low pressures (< or << 1
398 kbar), implying that their parent bodies were no larger than Vesta; the phase diagrams shown in
399 Fig. 5 thus provide a framework for estimating metamorphic conditions. Although no
400 compositional variables are strongly pressure dependent at these low pressures (Fig. 5), the
401 intersection between isopleths of two or more phases may improve existing constraints on
402 metamorphic pressures, leading to a better understanding of the size and thermal history of
403 meteorite parent bodies. However, potentially the most useful variable for constraining pressure
404 is Na in clinopyroxene, whose calculated values do not correspond well with measured
405 compositions, and that the solution models for both clinopyroxene and plagioclase may require
406 refinement.
407 Although minerals in type 7 ordinary chondrites may be compositionally zoned, they
408 preserve clear microstructural evidence for partial melting, implying temperatures in excess of
409 1050 °C. Following Tait et al. (2014), we consider type 7 meteorites as a simple continuation of
410 type 6, representing the extremes of thermal metamorphism in which temperatures exceeded the
411 dry silicate solidus.
412 The results presented here consider only isochemical pressure–temperature phase
413 diagrams. However, as low pressures can be assumed for most, or all, ordinary chondrites, the
414 approach may be used in the quantitative investigation of other variables. In particular: (i)

progressive oxidation during prograde metamorphism, which has been proposed to occur via volatilisation of hydrous matrix phases (Dunn et al., 2010b; McSween and Labotka, 1993), and; (ii) melt loss, the fundamental driver for differentiation of planetesimals to form the significant compositional diversity found in meteorites (Hutchison, 2004; Tait et al., 2014).

Acknowledgements

We are indebted to L. Nittler for sharing his database of meteorite bulk compositions. We acknowledge T. Dunn, E. Jennings and A. Tomkins for their thorough and generous reviews and B. Marty for his proficient editorial handling. Particular thanks to E. Jennings for help and discussions regarding the solution models used in the modelling. PAB acknowledges ARC support under the Australian Laureate Fellowship scheme.

Appendix A. Supplementary material

Supplementary material related to this article can be found online at: http://dx.doi.org/????.

References

Figure captions

Fig. 1. Binary variation diagram showing the composition of ordinary chondrites (darker shades are falls, paler shades are finds) in terms of MgO vs FeO. The average falls from each

441 compositional type (large symbols) define a linear relationship. Although type H chondrite have
442 the highest bulk Fe contents, they have on average the lowest FeO contents.
443
444 **Fig. 2.** Calculated isochemical *P–T* phase diagrams in the NCFMASCr model system showing
445 equilibrium assemblages in the average composition of (a) H, (b) L and (c) LL ordinary
446 chondrite falls from 0.001–15 kbar and 700–1200 °C. The absence of garnet and presence of
447 plagioclase and chromite in unmelted equilibrated ordinary chondrites constrains metamorphic
448 pressures to have been less than 8 kbar (i.e. to lie within the field with the emboldened
449 assemblage). The solidus (the onset of partial melting), indicated by the bold dashed line, occurs
450 at around 1050 °C at low pressures to around 1150 °C at 12 kbar where plagioclase is exhausted.
451 In (a) and (b), the fine dashed lines outline the fields within which two clinopyroxenes (relatively
452 Ca-rich and Ca–poor) coexist. The temperature ranges inferred for petrologic type 4–7
453 (equilibrated) chondrites based on two-pyroxene thermometry are shown (above each phase
454 diagram), in which types 4 and 5 are not differentiated (e.g. Tait et al., 2014).
455
456 **Fig. 3.** Phase diagrams from Fig. 2 contoured for the abundance (in mol.% normalised to one
457 oxygen) of the major silicate phases olivine (ol), orthopyroxene (opx), clinopyroxene (cpx) and
458 plagioclase (pl) in average H, L and LL ordinary chondrites from 0.001–15 kbar and 700–1200
459 °C. The measured mode of phases, in particular plagioclase and clinopyroxene, in ordinary
460 chondrites (Dunn et al., 2010a) demonstrates equilibration at low pressures. The white dashed
461 lines outline the fields where two clinopyroxenes (relatively Ca-rich and Ca–poor) coexist in
462 average H and L compositions, within which the abundance of clinopyroxene is a sum of both.
463
464 **Fig. 4.** Phase diagrams from Fig. 2b (L chondrites) contoured for mineral compositions. The
465 compositional variables for the minerals in the model system are defined as follows: in all phases
466 X(Fe) = Fe/(Fe + Mg); in pyroxenes X(Al) = 2 xAl^T = Al^T cations per formula unit (c.p.f.u.) on a

6 oxygen basis; in orthopyroxene $X(Ca) = xCa^{M2}$ = Ca c.p.f.u. (6 oxygen); in clinopyroxene $X(Na) = xNa^{M2}$ = Na c.p.f.u. (6 oxygen); in plagioclase $X(Ca)$ = mole fraction anorthite = Ca c.p.f.u. (8 oxygen); in chromite $X(Cr)$ = 3/2 Cr/(Fe + Mg + Al + Cr) = Cr/2 c.p.f.u. (4 oxygen); in which x is mole fraction, Al^T is tetrahedral Al, and Ca^{M2} and Na^{M2} are octahedral Ca and Na on the M2 site in pyroxene. The dashed lines in (g), (h) and (i) outline the fields where two clinopyroxenes coexist, within which the composition of clinopyroxene is an integrated composition combining both low-Ca and high-Ca clinopyroxene. The vertical grey bars show the range of measured compositions reported in Dunn et al. (2010b).

Fig. 5. Mineral compositions for L chondrites at low *P* (0.001–1 kbar). The compositional variables for the minerals in the model system are as follows: in all phases $X(Fe)$ = atomic Fe/(Fe + Mg); in pyroxenes $X(Al) = 2\ xAl^T = Al^T$ cations per formula unit (c.p.f.u.) on a 6 oxygen basis; in orthopyroxene $X(Ca) = xCa^{M2}$ = Ca c.p.f.u. (6 oxygen); in clinopyroxene $X(Na) = xNa^{M2}$ = Na c.p.f.u. (6 oxygen); in plagioclase $X(Ca)$ = mole fraction anorthite = Ca c.p.f.u. (8 oxygen); in chromite $X(Cr)$ = 3/2 Cr/(Fe + Mg + Al + Cr) = Cr/2 c.p.f.u. (4 oxygen); in which x is mole fraction, Al^T is tetrahedral Al, and Ca^{M2} and Na^{M2} are octahedral Ca and Na on the M2 site in pyroxene.

References

Allegre, C.J., Manhes, G., Göpel, C., 1995. The age of the Earth. Geochim. Cosmochim. Acta 59, 1445-1456.

Binns, R., 1970. Pyroxenes from non-carbonaceous chondritic meteorites. Mineral. Mag. 37, 649-669.

Bland, P.A., Cressey, G., Menzies, O.N., 2004. Modal mineralogy of carbonaceous chondrites by X-ray diffraction and Mössbauer spectroscopy. Meteorit. Planet. Sci. 39, 3-16.

Brearley, A.J., Jones, R.H., 1998. Chondritic meteorites. Rev. Mineral. Geochem. 36, 3.1-3.398.

Bunch, T.E., Keil, K., Snetsinger, K.G., 1967. Chromite composition in relation to chemistry and texture of ordinary chondrites. Geochim. Cosmochim. Acta 31, 1569-1582.

Ciesla, F.J., Davison, T.M., Collins, G.S., O'Brien, D.P., 2013. Thermal consequences of impacts in the early solar system. Meteorit. Planet. Sci. 48, 2559-2576.

Cressey, G., Schofield, P., 1996. Rapid whole-pattern profile-stripping method for the quantification of multiphase samples. Powder Diffr. 11, 35-39.

Dodd Jr, R.T., Schmus, W.R.V., Koffman, D.M., 1967. A survey of the unequilibrated ordinary chondrites. Geochim. Cosmochim. Acta 31, 921-934,IN921-IN924,935-951.

Dodd, R., Grover, J., Brown, G., 1975. Pyroxenes in the Shaw (L-7) chondrite. Geochim. Cosmochim. Acta 39, 1585-1594.

Dodd, R.T., 1969. Metamorphism of the ordinary chondrites: A review. Geochim. Cosmochim. Acta 33, 161-164,IN161-IN165,165-203.

Dodd, R.T., 1981. Meteorites, a petrologic-chemical synthesis. CUP Archive.

Dunn, T.L., Cressey, G., McSWEEN Jr, H.Y., McCOY, T.J., 2010a. Analysis of ordinary chondrites using powder X‐ray diffraction: 1. Modal mineral abundances. Meteorit. Planet. Sci. 45, 123-134.

509 Dunn, T.L., McSween Jr, H.Y., McCoy, T.J., Cressey, G., 2010b. Analysis of ordinary
510 chondrites using powder X-ray diffraction: 2. Applications to ordinary chondrite parent-
511 body processes. Meteorit. Planet. Sci. 45, 139-160.
512 Fitzsimons, I., Harley, S., 1994. The influence of retrograde cation exchange on granulite PT
513 estimates and a convergence technique for the recovery of peak metamorphic conditions. J.
514 Petrol. 35, 543-576.
515 Göpel, C., Manhès, G., Allègre, C.J., 1994. U–Pb systematics of phosphates from equilibrated
516 ordinary chondrites. Earth. Planet. Sci. Lett. 121, 153-171.
517 Green, E., Holland, T., Powell, R., 2012a. A thermodynamic model for silicate melt in CaO–
518 MgO–Al2O3–SiO2 to 50 kbar and 1800° C. J. Metamorph. Geol. 30, 579-597.
519 Green, E., Holland, T., Powell, R., White, R., 2012b. Garnet and spinel lherzolite assemblages in
520 MgO–Al2O3–SiO2 and CaO–MgO–Al2O3–SiO2: thermodynamic models and an
521 experimental conflict. J. Metamorph. Geol. 30, 561-577.
522 Harrison, K.P., Grimm, R.E., 2010. Thermal constraints on the early history of the H-chondrite
523 parent body reconsidered. Geochim. Cosmochim. Acta 74, 5410-5423.
524 Herndon, J., Herndon, M., 1977. Aluminum-26 as a planetoid heat source in the early solar
525 system. Meteoritics 12, 459-465.
526 Holland, T.J.B., Powell, R., 2011. An improved and extended internally consistent
527 thermodynamic dataset for phases of petrological interest, involving a new equation of
528 state for solids. J. Metamorph. Geol. 29, 333-383.
529 Huss, G.R., Rubin, A.E., Grossman, J.N., 2006. Thermal metamorphism in chondrites.
530 Meteorites and the early solar system II 943, 567-586.
531 Hutcheon, I.D., Hutchison, R., 1989. Evidence from the Semarkona ordinary chondrite for 26A1
532 heating of small planets. Nature 337, 238-241.
533 Hutchison, R., 2004. Meteorites: A petrologic, chemical and isotopic synthesis. Cambridge
534 University Press.

535 Jennings, E.S., Holland, T.J.B., 2015. A Simple Thermodynamic Model for Melting of Peridotite
536 in the System NCFMASOCr. J. Petrol. 56, 869-892.
537 Jurewicz, A., Mittlefehldt, D., Jones, J., 1993. Experimental partial melting of the Allende (CV)
538 and Murchison (CM) chondrites and the origin of asteroidal basalts. Geochim.
539 Cosmochim. Acta 57, 2123-2139.
540 Keil, K., 2000. Thermal alteration of asteroids: Evidence from meteorites. Planet. Space Sci. 48,
541 887-903.
542 Kelsey, D.E., Hand, M., 2015. On ultrahigh temperature crustal metamorphism: Phase equilibria,
543 trace element thermometry, bulk composition, heat sources, timescales and tectonic
544 settings. Geoscience Frontiers 6, 311-356.
545 Korhonen, F., Clark, C., Brown, M., Taylor, R., 2014. Taking the temperature of Earth's hottest
546 crust. Earth. Planet. Sci. Lett. 408, 341-354.
547 Mare, E.R., Tomkins, A.G., Godel, B.M., 2014. Restriction of parent body heating by
548 metal‐troilite melting: Thermal models for the ordinary chondrites. Meteorit. Planet. Sci.
549 49, 636-651.
550 McSween, H.Y., Patchen, A.D., 1989. Pyroxene thermobarometry in LL‐group chondrites and
551 implications for parent body metamorphism. Meteoritics 24, 219-226.
552 McSween Jr, H.Y., Labotka, T.C., 1993. Oxidation during metamorphism of the ordinary
553 chondrites. Geochim. Cosmochim. Acta 57, 1105-1114.
554 McSween Jr, H.Y., Sears, D.W.G., Dodd, R.T., 1988. Thermal metamorphism. Meteorites and
555 the early solar system, 102-113.
556 Minster, J.-F., Allègre, C.J., 1979. 87 Rb 87 Sr chronology of H chondrites: Constraint and
557 speculations on the early evolution of their parent body. Earth. Planet. Sci. Lett. 42, 333-
558 347.

559 Mittlefehldt, D.W., Lindstrom, M.M., 2001. Petrology and geochemistry of Patuxent Range
560 91501, a clast-poor impact-melt from the L chondrite parent body, and Lewis Cliff 88663,
561 an L7 chondrite. Meteorit. Planet. Sci. 36, 439-457.
562 Nittler, L.R., McCoy, T.J., Clark, P.E., Murphy, M.E., Trombka, J.I., Jarosewich, E., 2004. Bulk
563 element compositions of meteorites: A guide for interpreting remote-sensing geochemical
564 measurements of planets and asteroids. Antarct. Meteorit. Res. 17, 231.
565 Olsen, E.J., Bunch, T., 1984. Equilibration temperatures of the ordinary chondrites: A new
566 evaluation. Geochim. Cosmochim. Acta 48, 1363-1365.
567 Patterson, C., 1956. Age of meteorites and the earth. Geochim. Cosmochim. Acta 10, 230-237.
568 Pletchov, P.Y., Zinovieva, N., Latyshev, N., Granovsky, L., 2005. Evaluation of the
569 crystallization temperatures and pressures for clinopyroxene in the parental bodies of
570 ordinary chondrites, 36th Annual Lunar and Planetary Science Conference, p. 1041.
571 Powell, R., Holland, T.J.B., 1988. An internally consistent dataset with uncertainties and
572 correlations: 3. Applications to geobarometry, worked examples and a computer program.
573 J. Metamorph. Geol. 6, 173-204.
574 Rubin, A.E., 1990. Kamacite and olivine in ordinary chondrites: Intergroup and intragroup
575 relationships. Geochim. Cosmochim. Acta 54, 1217-1232.
576 Rubin, A.E., 1992. A shock-metamorphic model for silicate darkening and compositionally
577 variable plagioclase in CK and ordinary chondrites. Geochim. Cosmochim. Acta 56, 1705-
578 1714.
579 Rubin, A.E., 1995. Petrologic Evidence for Collisional Heating of Chondritic Asteroids. Icarus
580 113, 156-167.
581 Scott, E.R., Taylor, G.J., Keil, K., 1986. Accretion, metamorphism, and brecciation of ordinary
582 chondrites: Evidence from petrologic studies of meteorites from Roosevelt County, New
583 Mexico, Lunar and Planetary Science Conference Proceedings, p. 115.

584 Scott, E.R.D., 2007. Chondrites and the protoplanetary disk, Ann. Rev. Earth Planet. Sci., pp.
585 577-620.
586 Scott, E.R.D., Krot, T.V., Goldstein, J.I., Wakita, S., 2014. Thermal and impact history of the H
587 chondrite parent asteroid during metamorphism: Constraints from metallic Fe-Ni.
588 Geochim. Cosmochim. Acta 136, 13-37.
589 Scott, E.R.D., Rajan, R.S., 1981. Metallic minerals, thermal histories and parent bodies of some
590 xenolithic, ordinary chondrite meteorites. Geochim. Cosmochim. Acta 45, 53-67.
591 Slater-Reynolds, V., McSween Jr, H.Y., 2005. Peak metamorphic temperatures in type 6
592 ordinary chondrites: An evaluation of pyroxene and plagioclase geothermometry. Meteorit.
593 Planet. Sci. 40, 745-754.
594 Sleep, N.H., Zahnle, K.J., Kasting, J.F., Morowitz, H.J., 1989. Annihilation of ecosystems by
595 large asteroid impacts on the early Earth. Nature 342, 139-142.
596 Suess, H.E., 1965. Chemical evidence bearing on the origin of the solar system. Ann. Rev.
597 Astron. Astrophy. 3, 217.
598 Tait, A.W., Tomkins, A.G., Godel, B.M., Wilson, S.A., Hasalova, P., 2014. Investigation of the
599 H7 ordinary chondrite, Watson 012: Implications for recognition and classification of Type
600 7 meteorites. Geochim. Cosmochim. Acta 134, 175-196.
601 Trieloff, M., Jessberger, E.K., Herrwerth, I., Hopp, J., Fiéni, C., Ghélis, M., Bourot-Denise, M.,
602 Pellas, P., 2003. Structure and thermal history of the H-chondrite parent asteroid revealed
603 by thermochronometry. Nature 422, 502-506.
604 Urey, H.C., 1962. Life-Forms in meteorites: Origin of life-like forms in carbonaceous chondrites
605 introduction. Nature 193, 1119-1123.
606 Van Schmus, W., Wood, J.A., 1967. A chemical-petrologic classification for the chondritic
607 meteorites. Geochim. Cosmochim. Acta 31, 747-765.

White, R., Powell, R., Holland, T., Johnson, T., Green, E., 2014. New mineral activity–composition relations for thermodynamic calculations in metapelitic systems. J. Metamorph. Geol. 32, 261-286.

Zinovieva, N.G., Pletchov, P.Y., Latyshev, N.P., Granovsky, L.B., 2006. Thermobarometry of ordinary chondrites. Doklady Earth Sciences 409, 758-761.

Figure 1

Click here to download Figure: Fig 1 bulk compositions.pdf

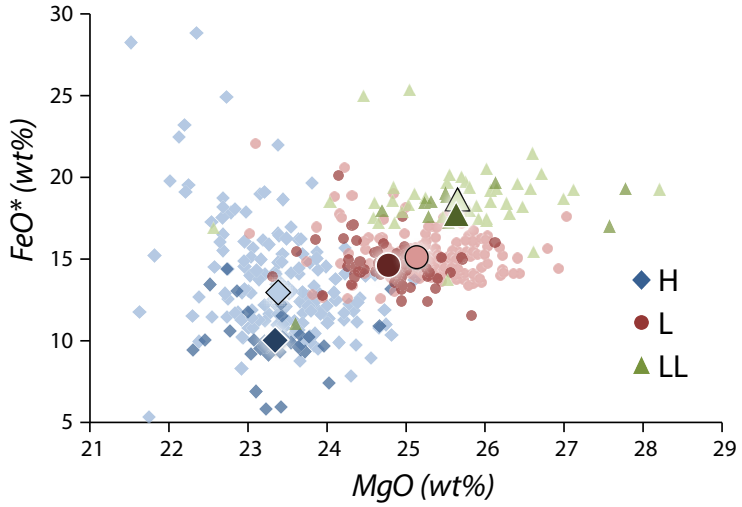

Fig. 1

Figure 2

Click here to download Figure: Fig 2 PT pseudosections.pdf

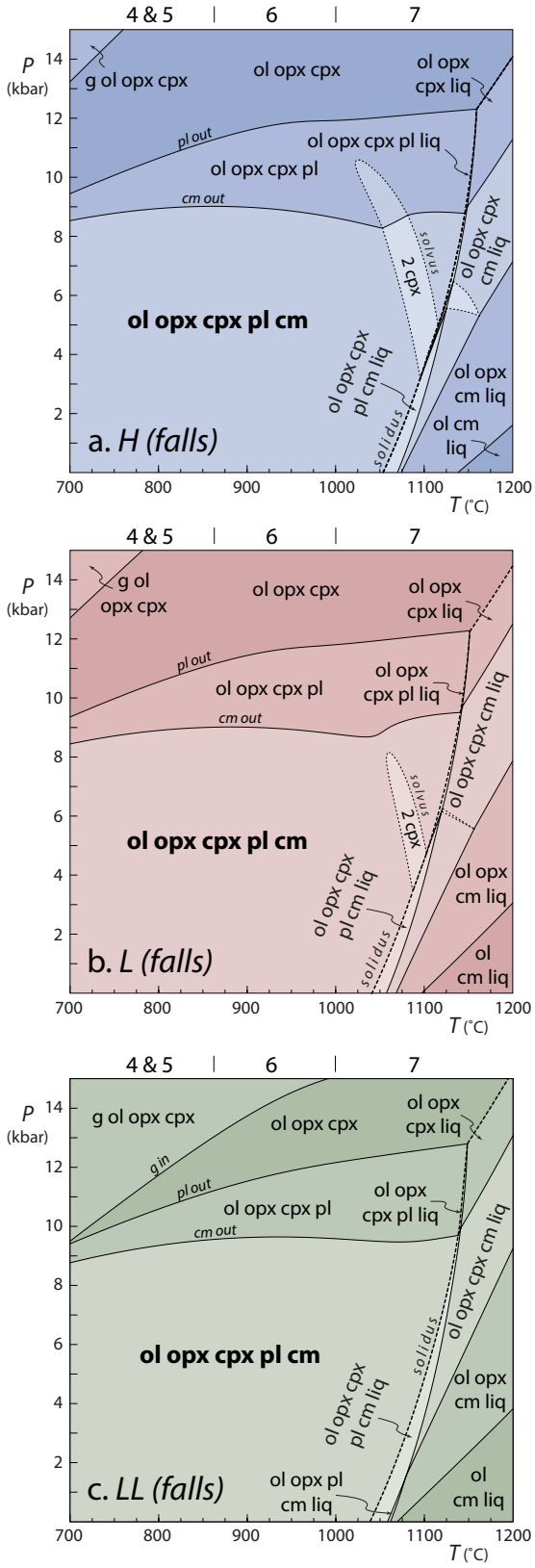

Fig. 2

Figure 3

Click here to download Figure: Fig 3 - modes to 15 kbar.pdf

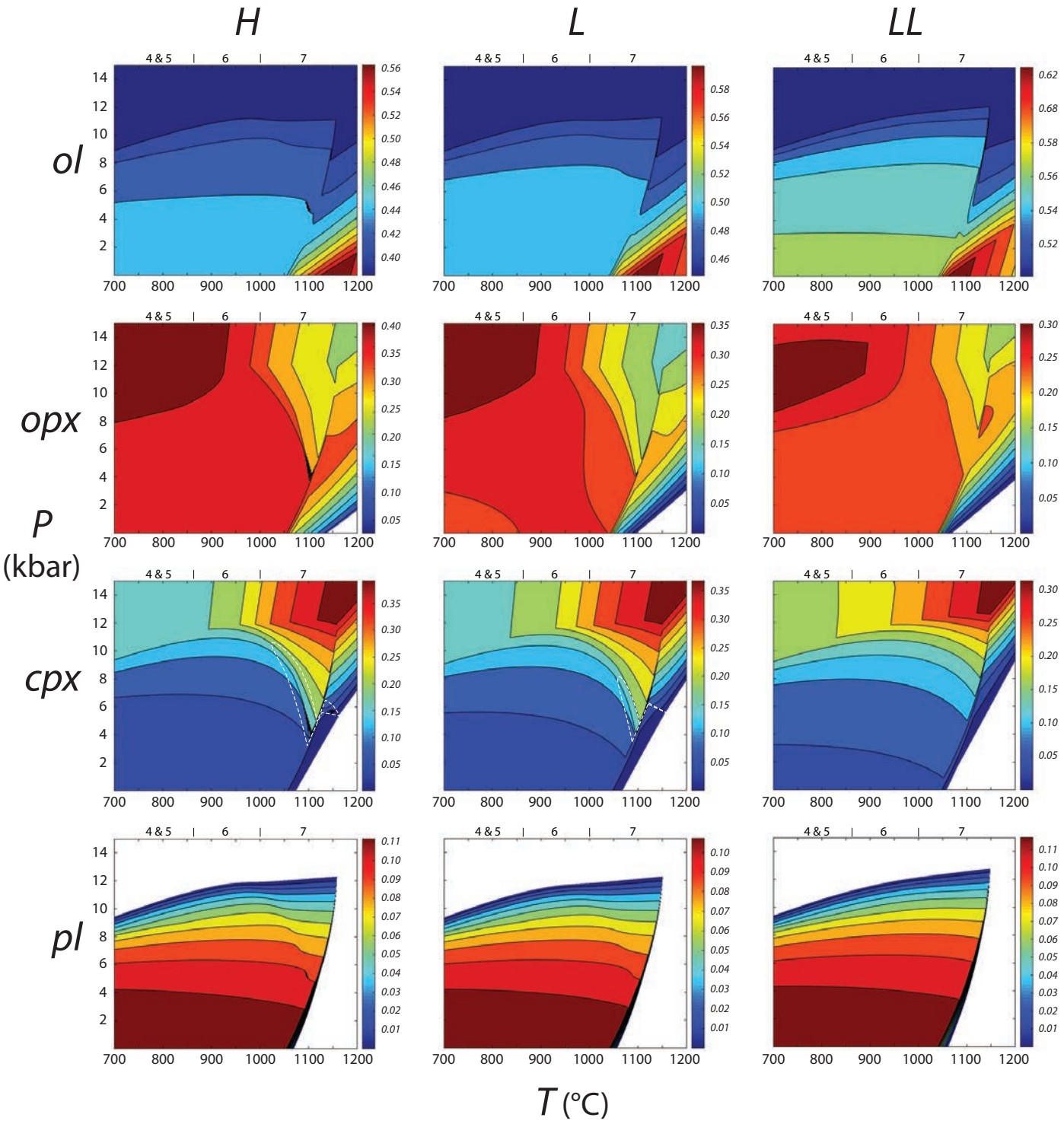

Fig. 3

Figure 4

Click here to download Figure: Fig 4 - min chem L_falls (to 15 kbar).pdf

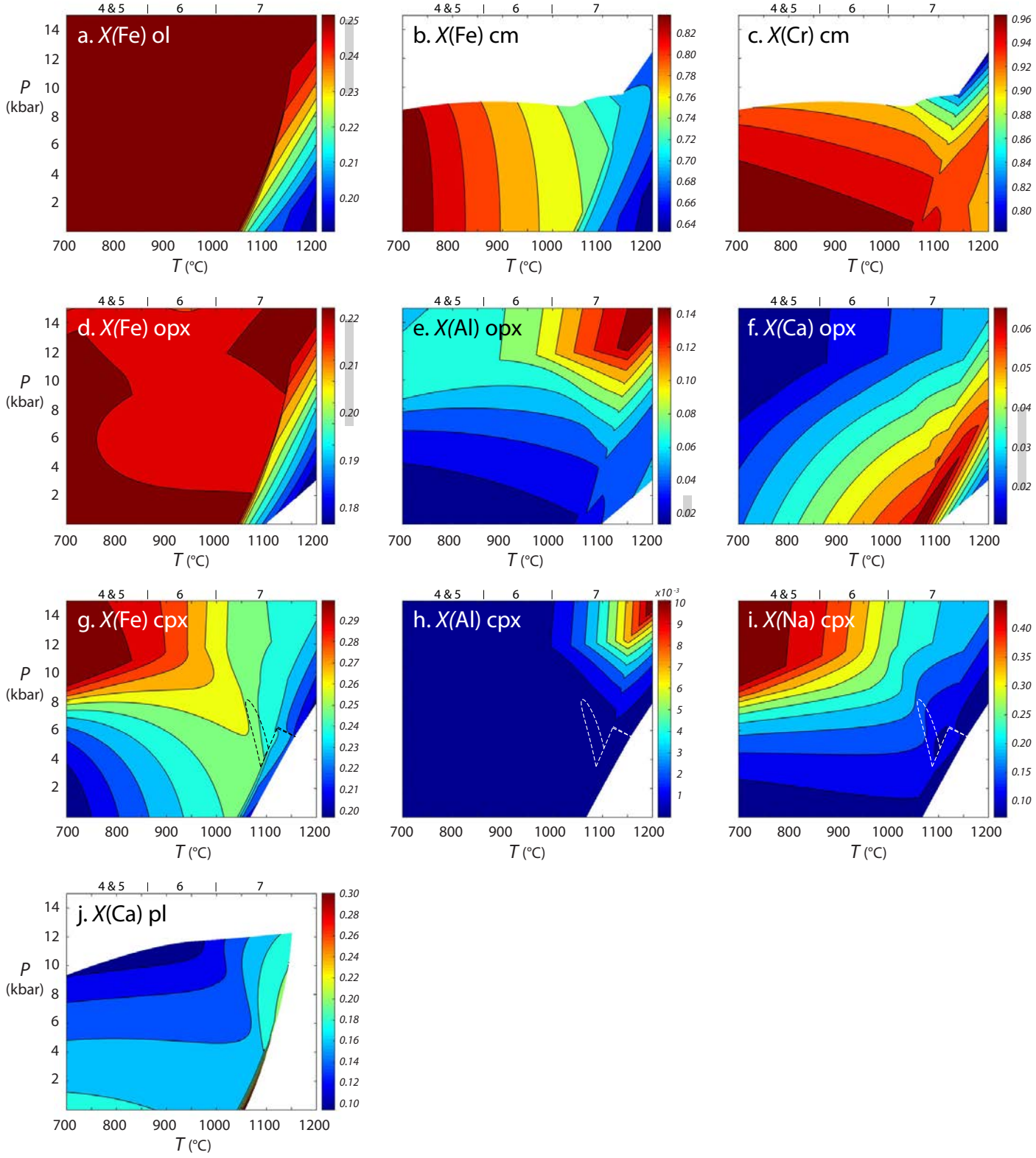

Fig. 4

Figure 5

Click here to download Figure: Fig 5 - min chem L_falls (to 1 kbar).pdf

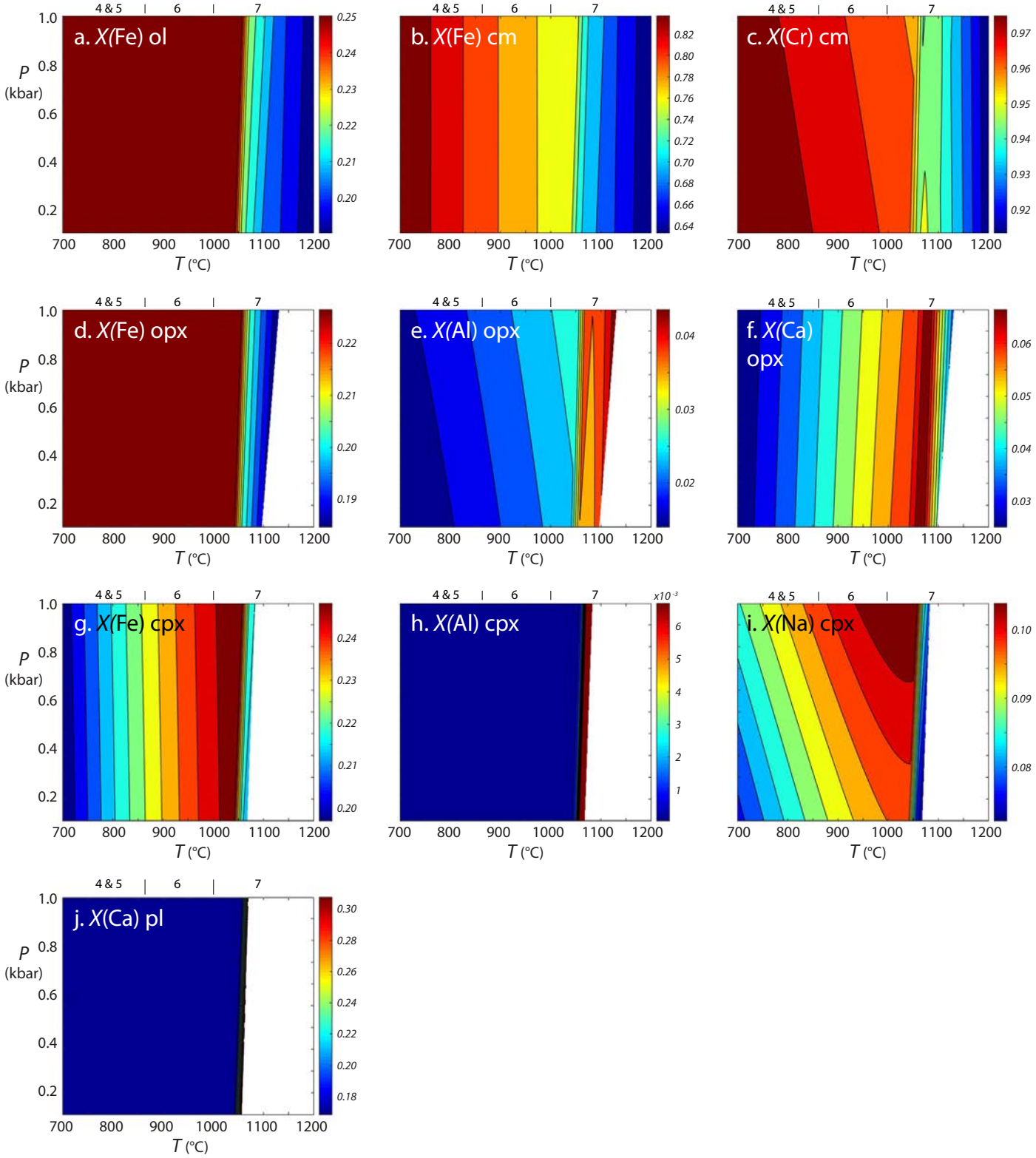

Fig. 5

Table

Click here to download Table: Table1.pdf

Table 1. Bulk compositions (mol.%) used in the construction of phase diagrams.

	SIO_2	FeO*	MgO	CaO	Al_2O_3	Cr_2O_3	Na_2O	SUM
H	43.746	10.057	41.653	1.770	1.542	0.234	0.998	100
L	42.675	13.159	39.753	1.771	1.447	0.217	0.977	100
LL	41.633	14.986	38.622	1.954	1.656	0.189	0.960	100

Table 2

Click here to download Table: Table2.pdf

	modes (wt%) normalised to 100%				compositions				
Type	ol	opx	cpx	pl	*X*(Fe) ol	*X*(Fe) opx	*X*(Al) opx	*X*(Ca) opx	*X*(Fe) cpx
H4	40.7	36.9	10.0	12.4	0.18	0.16	0.02	0.02	–
H5	44.5	33.9	9.7	12.0	0.19	0.17	0.01	0.03	–
H6	47.5	33.1	7.6	11.8	0.19	0.17	0.01	0.03	0.12
all H	**44.2**	**34.6**	**9.1**	**12.1**	**0.19**	**0.17**	**0.01**	**0.03**	**–**
L4	49.3	28.6	10.7	11.5	0.24	0.20	0.01	0.03	–
L5	50.6	29.0	9.2	11.2	0.25	0.21	0.01	0.03	–
L6	52.2	26.4	9.8	11.5	0.25	0.21	0.01	0.03	0.15
all L	**50.7**	**28.0**	**9.9**	**11.4**	**0.24**	**0.21**	**0.01**	**0.03**	**–**
LL4	55.5	25.2	8.5	10.8	0.28	0.23	0.03	0.05	–
LL5	57.0	24.3	8.0	10.7	0.29	0.24	0.01	0.03	–
LL6	59.2	21.3	8.5	11.0	0.30	0.25	0.01	0.03	0.17
all LL	**57.2**	**23.6**	**8.3**	**10.9**	**0.29**	**0.24**	**0.01**	**0.04**	**–**

Table 2. Measured mode and abundance of minerals in ordinary chondrites from Dunn et al. (2010a,b)